Nuclear Science and Engineering

ISSN: (Print) (Online) Journal homepage: https://www.tandfonline.com/loi/unse20

Blind Benchmark Exercise for Spent Nuclear Fuel Decay Heat

Peter Jansson, Martin Bengtsson, Ulrika Bäckström, Francisco Álvarez-Velarde, Dušan Čalič, Stefano Caruso, Ron Dagan, Luca Fiorito, Lydie Giot, Kevin Govers, Augusto Hernandez Solis, Volker Hannstein, Germina Ilas, Marjan Kromar, Jaakko Leppänen, Marita Mosconi, Pedro Ortego, Rita Plukienė, Arturas Plukis, Anssu Ranta-Aho, Dimitri Rochman, Linus Ros, Shunsuke Sato, Peter Schillebeeckx, Ahmed Shama, Teodosi Simeonov, Alexey Stankovskiy, Holly Trellue, Stefano Vaccaro, Vanessa Vallet, Marc Verwerft, Gašper Žerovnik & Anders Sjöland

To cite this article: Peter Jansson, Martin Bengtsson, Ulrika Bäckström, Francisco Álvarez-Velarde, Dušan Čalič, Stefano Caruso, Ron Dagan, Luca Fiorito, Lydie Giot, Kevin Govers, Augusto Hernandez Solis, Volker Hannstein, Germina Ilas, Marjan Kromar, Jaakko Leppänen, Marita Mosconi, Pedro Ortego, Rita Plukienė, Arturas Plukis, Anssu Ranta-Aho, Dimitri Rochman, Linus Ros, Shunsuke Sato, Peter Schillebeeckx, Ahmed Shama, Teodosi Simeonov, Alexey Stankovskiy, Holly Trellue, Stefano Vaccaro, Vanessa Vallet, Marc Verwerft, Gašper Žerovnik & Anders Sjöland (2022): Blind Benchmark Exercise for Spent Nuclear Fuel Decay Heat, Nuclear Science and Engineering, DOI: 10.1080/00295639.2022.2053489

To link to this article: https://doi.org/10.1080/00295639.2022.2053489

Published online: 29 Apr 2022.

NUCLEAR SCIENCE AND ENGINEERING

DOI: https://doi.org/10.1080/00295639.2022.2053489

Blind Benchmark Exercise for Spent Nuclear Fuel Decay Heat

Peter Jansson,[a]* Martin Bengtsson,[b] Ulrika Bäckström,[b] Francisco Álvarez-Velarde,[c] Dušan Čalič,[d] Stefano Caruso,[e,f] Ron Dagan,[g] Luca Fiorito,[h] Lydie Giot,[i] Kevin Govers,[j] Augusto Hernandez Solis,[h] Volker Hannstein,[k] Germina Ilas,[l] Marjan Kromar,[d] Jaakko Leppänen,[m] Marita Mosconi,[n] Pedro Ortego,[o] Rita Plukienė,[p] Arturas Plukis,[p] Anssu Ranta-Aho,[q] Dimitri Rochman,[r] Linus Ros,[s] Shunsuke Sato,[t] Peter Schillebeeckx,[u] Ahmed Shama,[e] Teodosi Simeonov,[v] Alexey Stankovskiy,[h] Holly Trellue,[w] Stefano Vaccaro,[x] Vanessa Vallet,[y] Marc Verwerft,[h] Gašper Žerovnik,[d,u] and Anders Sjöland[A,z]

[a] *Uppsala University, Uppsala, Sweden*
[b] *Vattenfall, Sweden*
[c] *Centro de Investigaciones Energéticas, MedioAmbientales y Tecnológicas (CIEMAT), Spain*
[d] *Jožef Stefan Institute, Ljubljana, Slovenia*
[e] *National Cooperative for the Disposal of Radioactive Waste (NAGRA), Switzerland*
[f] *NPP Gösgen-Däniken AG, Switzerland*
[g] *Karlsruhe Institute of Technology (KIT), Germany*
[h] *Belgian Nuclear Research Centre (SCK CEN), Belgium*
[i] *Université de Nantes, SUBATECH, CNRS-IN2P3, IMT-Atlantique, France*
[j] *Federal Agency for Nuclear Control (FANC), Belgium*
[k] *Gesellschaft für Anlagen- und Reaktorsicherheit (GRS), Germany*
[l] *Oak Ridge National Laboratory, Oak Ridge, Tennessee*
[m] *VTT Technical Research Centre of Finland Ltd, Finland*
[n] *DG Energy, EURATOM Safeguards, European Commission, Luxembourg*
[o] *SEA Ingenieria y Análisis de Blindajes S.L., Las Rozas, Madrid, Spain*
[p] *Center for Physical Sciences and Technology, Vilnius, Lithuania*
[q] *Teollisuuden Voima Oyj (TVO), Finland*
[r] *Paul Scherrer Institut, Switzerland*
[s] *DVel AB, Sweden*
[t] *Central Research Institute of Electric Power Industry (CRIEPI), Japan*
[u] *European Commission, Joint Research Centre (JRC), Geel, Belgium*
[v] *Studsvik Scandpower Inc, Newton, Massachusetts*
[w] *Los Alamos National Laboratory, Los Alamos, New Mexico*
[x] *Joint Research Centre (JRC), European Commission, Ispra, Italy*
[y] *Commissariat à l'Energie Atomique et aux Energies Alternatives (CEA), France*
[z] *Svensk Kärnbränslehantering AB (SKB), Sweden*
[A] *Lund University, Lund, Sweden*

Received October 5, 2021
Accepted for Publication March 11, 2022

*E-mail: peter.jansson@physics.uu.se

Abstract — *The decay heat rate of five spent nuclear fuel assemblies of the pressurized water reactor type were measured by calorimetry at the interim storage for spent nuclear fuel in Sweden. Calculations of the decay heat rate of the five assemblies were performed by 20 organizations using different codes and nuclear data libraries resulting in 31 results for each assembly, spanning most of the current state-of-the-art practice. The calculations were based on a selected subset of information, such as reactor operating history and fuel assembly properties. The relative difference between the measured and average calculated decay heat rate ranged from 0.6% to 3.3% for the five assemblies. The standard deviation of these relative differences ranged from 1.9% to 2.4%.*

Keywords — *Spent nuclear fuel, decay heat, calorimeter, experimental measure, validation.*

Note — *Some figures may be in color only in the electronic version.*

I. INTRODUCTION

Safe and economical management of spent nuclear fuel (SNF) requires an accurate estimation of the decay heat for different facilities involved in the SNF back-end chain, whatever the approach retained: dry or wet storage, disposal, or reprocessing. The safety and design assessments of these facilities define constraints on spent fuel assembly temperature and decay heat. Furthermore, front-end fuel cycle strategies can also be affected by back-end evaluations; i.e., fuel design and irradiation plans can be optimized under the perspective of SNF key management issues. Therefore, a key point for optimizing the process of managing SNF relates to how well decay heat can today be estimated for a wide range of spent fuel assembly characteristics. Bias and uncertainties in decay heat estimation call for provision margins with regard to the facility optimization, its design, and the conformity requirement on the SNF acceptance criteria. In turn, this has an impact on the cost of the individual facilities and on the global cost of SNF management.

At present, computer codes and associated nuclear data (ND) libraries are validated against available measurements or integral experiments that cover a limited space of SNF assembly characteristics. The level of detail in assembly design and operating data that is required for accurate calculations often exceeds what is available, from an industrial perspective, for the whole SNF inventory arising from reactor operations. A bias in the calculated decay heat rate that is introduced due to the unavailability of such details in the input data can be assessed by performing sensitivity studies. However, as these evaluations depend on the computational tool and model, a deeper understanding can be gained through benchmark exercises involving different computer codes and users, which might lead to improved computational methods.

Therefore, the Swedish Nuclear Fuel and Waste Management Company (SKB) organized and coordinated a blind test benchmark exercise addressing both code-to-code and code-to-experiment comparisons. The dual purposes of the benchmark exercise consist of (1) comparing the blind predictions obtained from different simulation codes and users with experimental data and (2) studying the influence of the design characteristics and operation history on the calculated results.

An extra, implicit purpose of this blind test was to demonstrate the capability of the current state-of-the-art calculations of decay heat rate to reproduce the measured decay heat rate values of SNF assemblies using a set of input data that can be considered to be realistically available and under control for operators of facilities.

Many of the participants in this exercise are also collaborating within the work package Spent Fuel Characterization and Evolution until Disposal (SFC) in the context of the European Joint Programme on Radioactive Waste Management (EURAD) and in the International Atomic Energy Agency (IAEA) Coordinated Research Project on SNF characterization. The results of this blind test benchmark exercise will provide valuable input to such collaborative work and will contribute to a better characterization of SNF.

All uncertainties provided are quoted at a 68% confidence level unless otherwise stated. The notation $\langle x \rangle$ used in this paper denotes the average of x. Values including uncertainties are given in standard compact notation, such as V(U) where U indicates the uncertainty in the last digit(s) of V.

II. CHRONOLOGY AND BENCHMARK EXERCISE PROCEDURE

Several meetings were held to establish the procedure and to discuss the results of the blind test:

1. *September 18–19, 2017, Uppsala, Sweden*: At an initial meeting about the proposal of the SFC work

package of EURAD, the idea of conducting the blind test was presented by SKB. Several participants were interested and the idea was conveyed to others.

2. *October 27, 2017, Joint Research Centre (JRC)–Geel, Belgium*: A preparatory meeting was held in conjunction with a training course, "From nuclear data to a reliable estimate of spent fuel decay heat," organized by the JRC-Geel and the Belgian Nuclear Research Centre (SCK CEN).

3. *April 6, 2018, Paris, France*: Participants were invited to a meeting hosted by the Organisation for Economic Co-operation and Development/Nuclear Energy Agency (OECD/NEA). It was decided, with consensus, which input data should be provided to the participants and that the decay heat and content of ^{137}Cs and ^{148}Nd should be calculated for each fuel assembly. The content of the nuclides ^{137}Cs and ^{148}Nd were selected since these are good indicators of burnup (BU), being produced during irradiation as fission products without a complicated chain of neutron captures.

4. *July 1, 2019, Paris, France*: The OECD/NEA hosted a fourth meeting where the results of the calculations were presented after anonymization. Measured decay heat values were also presented.

5. *September 2019*: An error in the average assembly power used as input data was discovered for all five fuel assemblies. An arithmetic mean had been used instead of an energy-integrated average calculation of the assembly power based on rodwise power values.

6. *October 2019*: Updated input data were provided to the participants.

7. *November 2019*: The evaluation of the measured decay heat values was updated after it was discovered that a wrong electric power sensor of the calorimeter was used in the evaluation.

8. *December 20, 2019*: Updated values on measured decay heat were provided to the participants. A late participant to the blind test joined after December 20, 2019, but without access to the measured decay heat values before the calculated results were provided.

9. *2020 to May 2021*: Quality assurance procedures applied to the method to determine the calorimetric measurements resulted in a revised method and uncertainty quantification with a corresponding small update of the calorimetric results.

The blind test benchmark exercise comprises a set of five fuel assemblies from a pressurized water reactor (PWR) nuclear power plant in Sweden. These fuel assemblies have different materials, operation histories, and cooling times (CTs). Table I summarizes the BU, CT, and initial enrichment (IE) of these fuel assemblies. The fuel assemblies are of the 17 × 17 design with 264 fuel rods, 24 guide tubes, and a central instrumentation tube. In Table I, BU, IE, and CT refer to the assembly average BU, IE (^{235}U weight fraction in U), and CT in years (the difference between the time of achieved subcriticality after the last irradiation cycle in the reactor and the time of the calorimetric measurement), respectively. The fuel assembly identified as BT03 had Gd burnable absorbers (BAs) with IE 2.80% for the central part with eight rods. Note that the BU values listed in Table I were not used as input in this exercise.

Twenty different organizations have participated in the blind test benchmark exercise. Each participant has reported blind results that were compared to the values determined by the calorimetric measurements. Since some of the participants used more than one code/ND library, more calculated values than the number of participants have been reported for each of the five fuel assemblies.

III. MEASUREMENTS OF DECAY HEAT BY CALORIMETRY

Full-length calorimetric measurements of the fuel assemblies have been conducted at the Central Interim Storage Facility for Spent Nuclear Fuel (Clab) in Sweden, operated by SKB. Figure 1 shows the calorimeter. The temperature rising method to determine the thermal power was used, in which the thermal power inside the calorimeter is proportional to the temperature increase rate at the onset of identical temperature between the calorimeter and its environment (i.e., under adiabatic conditions). Two corrections are applied: (1) a correction for the difference in specific heat capacity of the calorimeter and the one of the electrical heater to calibrate the calorimeter and (2) a correction for gamma-ray heating outside of the calorimeter by means of additional dose rate measurements.

Uncertainties from the model used in the calibration fitting procedure as well as uncertainties in measured data were used in uncertainty propagation, including covariances

TABLE I

Fuel Assemblies Included in the Exercise and Their Basic Parameters with Data from Ref. 1

Identification	BU (GWd/tU)	CT (a)	IE (%)
BT01	53	4.5	3.95
BT02	55	8.6	3.95
BT03	50	9.8	3.95
BT04	51	13.5	3.70
BT05	50	21.4	3.60

Fig. 1. Photo of the calorimeter used for measurements of decay heat at the Clab.

where applicable. A conservative estimate of the uncertainty for the difference in specific heat capacity is 5%. At present, this is the largest contribution to the uncertainty of the measured decay heat rate, which is a common uncertainty component. For details, the reader is referred to Ref. 2.

Reference 3 describes the methodology to derive the decay heat rate from raw calorimetric data, while Ref. 2 addresses the uncertainty calculations. The raw data from the calorimetric measurements of the fuel assemblies in the benchmark exercise, available from Ref. 1, were used for this exercise. Four of the calibration measurements from Ref. 1 contained measurement data for the complete cool-down and heat-up cycle of the calorimeter, but only the data logged in the measurement time interval corresponding to the heat-up part[a] were used here. Besides this, the raw data from Ref. 1 were used unaltered as input data. Figure 2 displays the calorimetric calibration curve established using these data.

The results from the calorimetric measurements are listed in Table II. A correction factor of 0.915(46) for the differences in mass of the fuel assemblies compared to the mass of the electrically heated model from Ref. 4 was used. The loss in the decay heat rate due to gamma rays escaping from the calorimeter was estimated from measurements with a diode dose rate sensor positioned about 33 cm outside the calorimeter in the water pool. Uncertainties listed in Table II contain a conservative estimate of the uncertainty in both the mass difference correction as well as the one of the gamma correction.

IV. DATA PROVIDED AS INPUT FOR CALCULATIONS OF DECAY HEAT

All participants performed calculations based on the reactor data and fuel assembly design and irradiation history as provided by the SKB organizers.

Core data from one PWR-type reactor in Sweden were provided, addressing the reactor coolant system pressure,

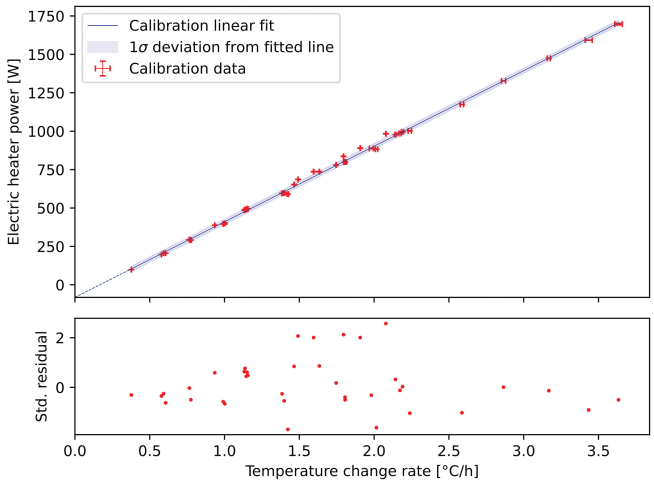

Fig. 2. Calorimetric calibration curve established using data published in Ref. 1.

[a] The files were named (a) EV_ 600W_2017-04-12.xlsx, (b) EV_900W_2017-04-13.xlsx, (c) EV_1000W_2017-04-18.xlsx, and (d) EV_1000W_2017-10-03.xlsx in Ref. 1. The used time intervals, in seconds, were between 10^4 and 3.5×10^4 for (a), after 8×10^3 for (b), after 2.0×10^4 for (c), and after 1.2×10^4 for (d).

TABLE II

Estimated Gamma-Ray Escape Heat Rate and Experimental Fuel Assembly Decay Heat Rate After Correction for the Difference in Mass of Assembly and Electrical Heater and for Heat Loss Due to Gamma-Rays Escaping from the Calorimeter

Identification	Gamma-Ray Escape Heat Rate (W)	Decay Heat Rate (W)
BT01	58(10)	1662(85)
BT02	30(5)	1068(56)
BT03	21(4)	895(48)
BT04	15(3)	768(42)
BT05	12(2)	663(37)

number of fuel assemblies in the core assembly pitch, active core height, and number of control rods in the core.

IV.A. Operational History

The provided data addressed cycle length and down time between the cycles; cycle-average assembly power; cycle-average core coolant temperature; fuel temperatures; soluble boron concentration in the coolant at beginning, middle, and end of cycle; and the assembly position in the core. Average fuel temperature refers to the average fuel temperature in the core for the specific cycle. This is an output value from CASMO-5/Simulate-3 calculations. Table III specifies the information about the operational history of the fuel assemblies that was provided to the participants.

The average power was calculated with CASMO-5/Simulate-3 with versions CASMO5-2.08.00 with ENDF/B-VII (e7r1.202.586) and SIMULATE-3 6.09.33_VAT_14, INTERPIN-4.01, and CMSLINK5-1.07.02. These calculations were performed by the reactor physics department at the Ringhals nuclear power plant in Sweden using a condensed operation history based on the following listed information. The list indicates the level of uncertainties on the data used as input to the reactor core calculations used to provide input data used in this exercise:

1. in-core measurement of the thermal neutron flux at full power, all control rods withdrawn and under xenon equilibrium (The calculated neutron flux, i.e., the solution of the diffusion equation in Simulate-3, is corrected based on monthly measurements of the neutron flux in approximately 3000 positions in the reactor core. The uncertainty in the measured neutron flux is in the order of 3%.)
2. the control rod history
3. the temperature of the water input to the reactor core

TABLE III

Duration of Each Irradiation Cycle, Subcritical Periods Between the Cycles, and Average Assembly Power

Identification	Cycle	Power Operation (days)	Subcritical (days)	Average Assembly Power (MW)
BT01	1	335	164	18.70
	2	274	47	21.14
	3	233	28	21.06
	4	417	1637	18.14
BT02	1	337	26	19.10
	2	296	26	21.85
	3	317	360	18.13
	4	389	3142	16.97
BT03	1	337	26	23.37
	2	296	26	22.05
	3	317	28	18.67
	4	308	3567	9.04
BT04	1	340	23	16.59
	2	324	28	19.67
	3	332	2592	17.78
	4	313	4925	17.27
BT05	1	329	48	18.66
	2	340	23	18.28
	3	324	28	17.33
	4	332	7826	15.41

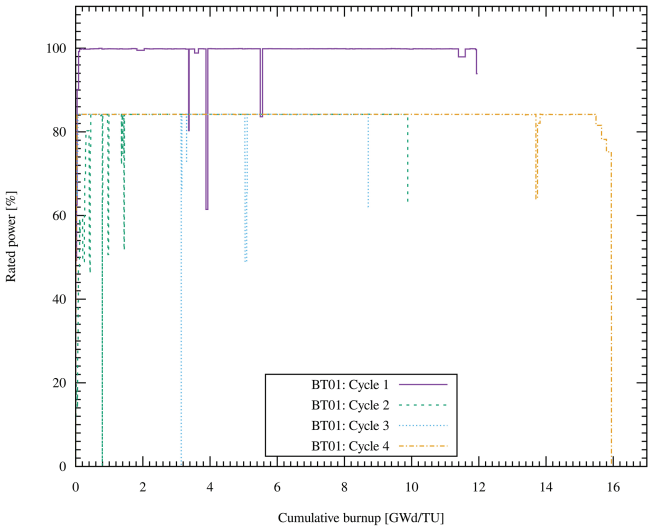

Fig. 3. Rated power versus cumulative BU per cycle in the fuel assembly BT01.

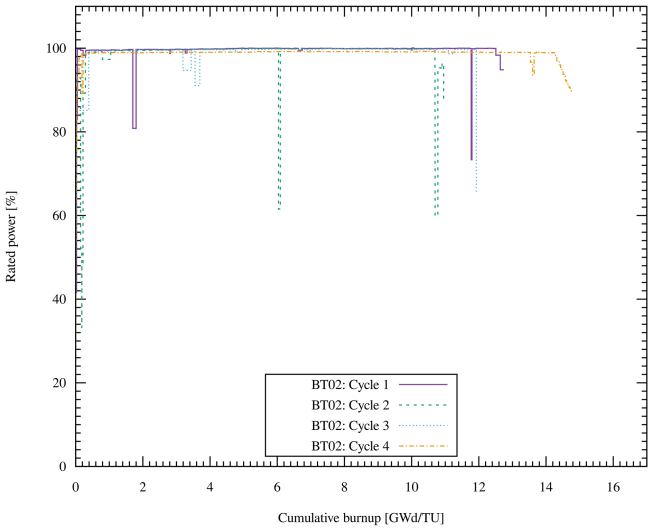

Fig. 4. Rated power veersus cumulative BU per cycle in the fuel assembly BT02.

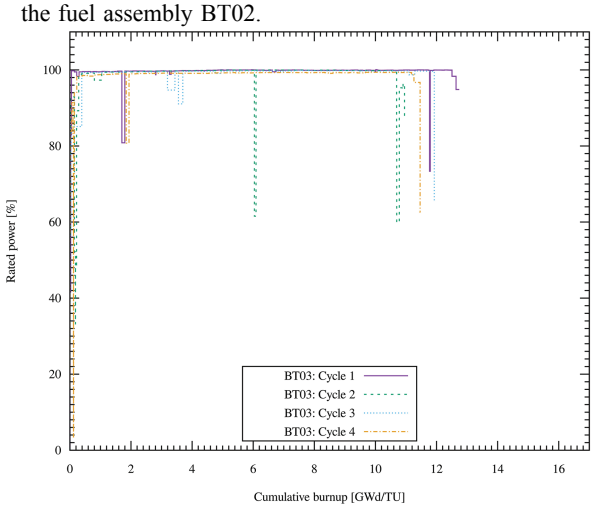

Fig. 5. Rated power versus cumulative BU per cycle in the fuel assembly BT03.

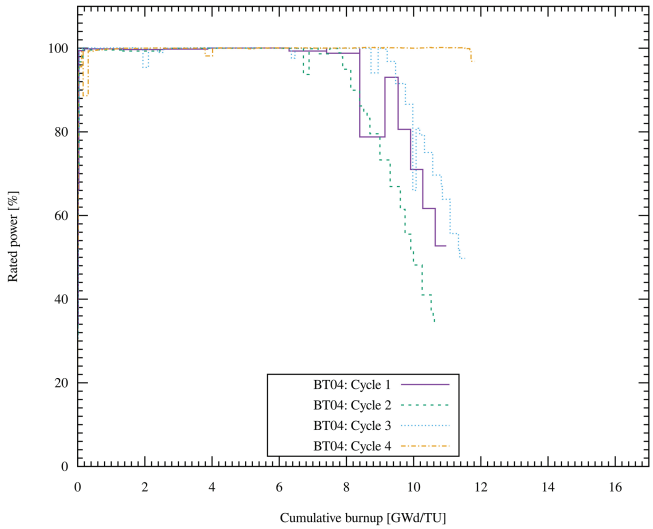

Fig. 6. Rated power versus cumulative BU per cycle in the fuel assembly BT04.

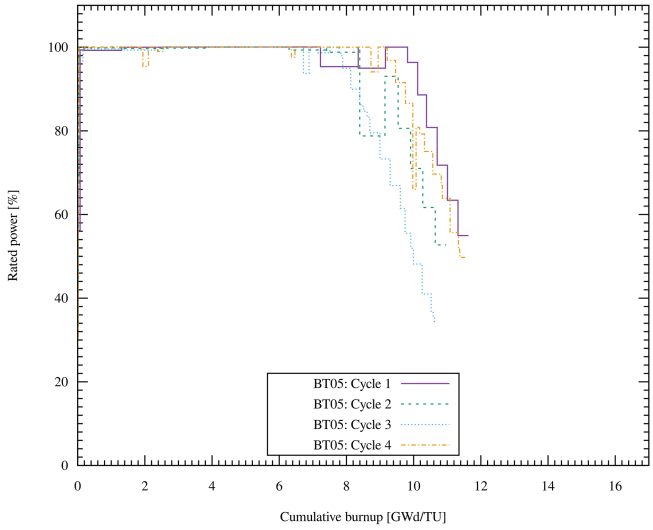

Fig. 7. Rated power versus cumulative BU per cycle in the fuel assembly BT05.

4. the thermal power of the reactor with an estimated uncertainty in the order of 2%.

The calculated neutron flux is used, together with the relative core power and the recoverable energy per fission, to calculate the relative nodal power distribution of the core. The relative core power includes decay heat at nominal power, including gamma power.

Figures 3 through 7 illustrate the detailed operational power history of the fuel assemblies. In Figs. 3 through 7, rated power is defined as the fraction of the licensed full power of the reactor. This information was not disclosed to the participants of the blind test, but averaged power values together with the power operation period as listed in Table III were given.

IV.B. Fuel Assembly Data

The following data were provided to the participants: manufacturer, fuel assembly model, initial weight of heavy metal, IE, pellet mass density, number of fuel rods with BAs, BA content, average IE for the fuel assembly with BA, cladding material name, spacer material, spacer linear mass density, spacer volumetric mass density, geometry of the pellets, claddings, guide tubes, and fuel assembly.

V. CODES AND ND LIBRARIES

Participants to the blind test benchmark exercise used different depletion tools and ND libraries, as listed in Table IV. The order of the codes and libraries listed in Table IV do not correspond to the identifiers used for presenting results. The Appendix provides details regarding the different procedures that were followed for each calculation.

VI. RESULTS FROM CALCULATIONS OF DECAY HEAT AND COMPARISON TO MEASUREMENTS

The calculated results are presented in Tables V through IX. They compare the measured and calculated decay heat rate for each assembly as well as calculated values of the content of ^{137}Cs and ^{148}Nd. Figure 8 illustrates the relative difference between the measured and calculated decay heat rate. The shaded background with a black border in Fig. 8 indicates the average estimated uncertainty of the measur ements.

The relationship between the nuclide inventory and decay heat are the half-lives and Q-values (released heat per decay). The Q-values can also be understood as the values of energy released from the decaying nuclides which are provided in the decay data libraries. Different Q-values were used in different calculations, depending on the code and library used. Some details on the used Q-values are given in the Appendix for the various codes.

TABLE IV

Codes and Evaluated ND Libraries Used by Participants in the Blind Test Benchmark Exercise

Code	Library	Appendix Section
ALEPH 2.7.2	ENDF/B-VII.1	A.I.A
APOLLO2.8/DARWIN2.3	JEFF-3.1.1	A.I.B
CASMO-4E + ORIGEN-S	JEF-2.2	A.I.C
CASMO-5 (2.03)	ENDF/B-VII.1	A.I.D
CASMO-5 (2.12.00) + SNF (1.07.02)	ENDF/B-VII.1	A.I.E
DRAGON 4.0.5	ENDF/B-VII.1	A.I.F
EVOLCODE (MCNP + ACAB)	JEFF-3.3	A.I.G
MCNP-CINDER + Nukleonika (2D)	ENDF/B-VII.1	A.I.H
Monteburnsv3 + CINDER	ENDF/B-VII.1	A.I.I
MOTIVE (KENO-VI + VENTINA)	ENDF/B-VII.1	A.I.J
MOTIVE (OpenMC + VENTINA)	ENDF/B-VIII	A.I.K
MVP 3	ENDF/B-VII.1	A.I.L
MVP 3	JEFF-3.2	A.I.M
MVP 3	JENDL-4.0	A.I.N
OREST	JEF-2.2 + ENDF/B-VI	A.I.O
SCALE 6.0: ORIGEN-ARP	ENDF/B-V	A.I.P
SCALE 6.1.3: ORIGEN-ARP	ENDF/B-V	A.I.Q
SCALE 6.2.3: ORIGAMI	ENDF/B-VII.1	A.I.P
SCALE 6.2.3: Polaris	ENDF/B-VII.1	A.I.R
SCALE 6.2.3: ORIGEN	ENDF/B-VII.1	A.I.R
SCALE 6.2.3: TRITON/KENO	ENDF/B-VII.1	A.I.S
SCALE 6.2.3: TRITON/NEWT	ENDF/B-VII.1	A.I.T
SEADEP	JEFF-3.1.1	A.I.U
Serpent 2.1.29	ENDF/B-VII.1	A.I.V
Serpent 2.1.29	JEFF-3.1.1	A.I.W
Serpent 2.1.31	JEFF-3.2 + JEFF-3.1.1	A.I.X

TABLE V

Calculated (C) and Measured (E) Decay Heat Rate and Mass of ^{137}Cs and ^{148}Nd for Fuel Assembly BT01

Calculation Identification	Decay Heat Rate				^{137}Cs		^{148}Nd	
	C (W)	$E - C$ (W)	$\frac{E-C}{E}$ (%)	$\frac{\langle C\rangle - C}{\langle C\rangle}$ (%)	Mass (g)	$\frac{\langle C\rangle - C}{\langle C\rangle}$ (%)	Mass (g)	$\frac{\langle C\rangle - C}{\langle C\rangle}$ (%)
1	1593	69	4.2	1.7	797	0.1	271	0.6
2	1630	32	1.9	−0.6	796	0.3	272	0.1
3	1627	35	2.1	−0.5	792	0.8	271	0.6
4	1638	24	1.4	−1.1	797	0.1	276	−1.1
5	1584	78	4.7	2.2	806	−1.0	271	0.7
6	1612	50	3.0	0.5	803	−0.6	274	−0.4
7	1586	76	4.6	2.1	797	0.1	276	−1.2
8	1618	44	2.7	0.1	773	3.2	267	2.1
9	1554	108	6.5	4.1	795	0.4	273	−0.1
10	1602	60	3.6	1.1	802	−0.4	275	−0.9
11	1634	28	1.7	−0.9	802	−0.5	275	−1.0
12	1696	−34	−2.0	−4.7	804	−0.7	273	0.0
13	1696	−34	−2.1	−4.7	809	−1.4	279	−2.2
14	1611	51	3.1	0.6	800	−0.2	274	−0.6
15	1608	54	3.2	0.7	799	−0.1	274	−0.5
16	1587	75	4.5	2.0	806	−1.0	271	0.7
17	1611	51	3.1	0.5	793	0.7	276	−1.2
18	1609	53	3.2	0.6	802	−0.4	274	−0.3
19	1605	57	3.4	0.9	803	−0.5	274	−0.4
20	1640	22	1.3	−1.2	805	−0.9	274	−0.6
21	1621	41	2.5	−0.1	799	−0.1	273	0.0
22	1610	52	3.1	0.6	800	−0.2	273	−0.1
23	1693	−31	−1.9	−4.5	787	1.4	270	0.9
24	1589	73	4.4	1.9	795	0.5	271	0.6
25	1635	27	1.6	−0.9	797	0.2	270	1.0
26	1611	51	3.1	0.5	797	0.1	272	0.3
27	1603	59	3.5	1.0	797	0.2	271	0.5
28	1634	28	1.7	−0.9	797	0.2	270	1.0
29	1634	28	1.7	−0.9	797	0.2	270	1.0
30	1633	29	1.7	−0.8	797	0.2	270	1.0
31	1612	50	3.0	0.5	803	−0.6	274	−0.4
Average	1620	42	2.5	0	798	0	273	0
Standard deviation	32	32	1.9	2.0	7	0.8	2	0.9

TABLE VI

Calculated (C) and Measured (E) Decay Heat Rate and Mass of ^{137}Cs and ^{148}Nd for Fuel Assembly BT02

Calculation Identification	Decay Heat Rate				^{137}Cs		^{148}Nd	
	C (W)	$E - C$ (W)	$\frac{E-C}{E}$ (%)]	$\frac{\langle C\rangle - C}{\langle C\rangle}$ (%)	Mass (g)	$\frac{\langle C\rangle - C}{\langle C\rangle}$ (%)	Mass (g)	$\frac{\langle C\rangle - C}{\langle C\rangle}$ (%)
1	1027	41	3.9	1.6	734	0.4	279	0.8
2	1048	20	1.8	−0.5	732	0.7	279	0.6
3	1042	26	2.4	0.1	727	1.3	278	1.1
4	1040	28	2.6	0.3	733	0.5	283	−0.7
5	1034	34	3.2	0.9	743	−0.8	279	0.9
6	1045	23	2.1	−0.2	738	−0.2	281	0.0
7	1012	56	5.3	3.1	734	0.4	283	−0.8
8	1041	27	2.5	0.2	694	5.9	266	5.5
9	1046	22	2.1	−0.2	755	−2.5	291	−3.5
10	1021	47	4.4	2.1	750	−1.8	287	−2.2
11	1049	19	1.8	−0.5	750	−1.8	288	−2.3
12	1082	−14	−1.3	−3.7	751	−2.0	285	−1.3
13	1099	−31	−2.9	−5.3	746	−1.2	287	−2.1
14	1031	37	3.4	1.2	739	−0.2	283	−0.7
15	1024	44	4.1	1.9	736	0.1	282	−0.3
16	1037	31	2.9	0.6	743	−0.8	279	0.9
17	1016	52	4.9	2.6	732	0.7	285	−1.2
18	1041	27	2.5	0.2	739	−0.3	282	−0.2
19	1042	26	2.5	0.2	739	−0.3	281	−0.1
20	1064	4	0.3	−2.0	738	−0.1	282	−0.3
21	1026	42	3.9	1.7	737	0.0	280	0.2
22	1040	29	2.7	0.4	737	−0.0	281	0.2
23	1093	−25	−2.4	−4.8	725	1.6	278	1.1
24	1033	35	3.2	1.0	736	0.1	280	0.3
25	1052	16	1.5	−0.8	736	0.1	278	0.9
26	1043	25	2.3	0.0	736	0.1	281	0.2
27	1026	42	3.9	1.7	736	0.1	280	0.5
28	1052	16	1.5	−0.8	736	0.1	278	0.9
29	1050	18	1.7	−0.6	736	0.1	278	0.9
30	1050	18	1.7	−0.6	736	0.1	278	0.9
31	1040	28	2.6	0.3	740	−0.4	282	−0.2
Average	1043	25	2.3	0	737	0	281	0
Standard deviation	20	20	1.8	1.9	10	1.4	4	1.5

TABLE VII

Calculated (C) and Measured (E) Decay Heat Rate and Mass of ^{137}Cs and ^{148}Nd for Fuel Assembly BT03

Calculation Identification	Decay Heat Rate				^{137}Cs		^{148}Nd	
	C (W)	$E - C$ (W)	((%)	$\frac{\langle C\rangle - C}{\langle C\rangle}$ (%)	Mass (g)	$\frac{\langle C\rangle - C}{\langle C\rangle}$ (%)	Mass (g)	$\frac{\langle C\rangle - C}{\langle C\rangle}$ (%)
1	857	38	4.3	1.0	662	0.0	255	0.6
2	866	29	3.2	−0.1	635	4.1	247	3.9
3	865	30	3.4	0.1	655	1.2	255	0.8
4					728	−9.9	286	−11.3
5	864	31	3.4	0.2	670	−1.2	256	0.5
6	871	24	2.7	−0.6	666	−0.5	258	−0.4
7	844	52	5.8	2.5	663	−0.1	260	−1.4
8	869	26	3.0	−0.4	627	5.4	245	4.8
9	822	73	8.2	5.0	649	2.0	254	1.1
10	847	48	5.3	2.1	665	−0.4	259	−0.9
11	873	22	2.4	−0.9	666	−0.5	260	−1.0
12	882	13	1.5	−1.9	668	−0.8	258	−0.3
13	917	−22	−2.4	−5.9	670	−1.2	262	−2.1
14	853	42	4.7	1.4	663	−0.1	258	−0.6
15	851	44	4.9	1.7	664	−0.2	258	−0.4
16	867	28	3.1	−0.2	670	−1.2	256	0.5
17	843	52	5.8	2.6	658	0.7	260	−1.1
18	878	17	1.9	−1.4	660	0.4	255	0.6
19	870	25	2.8	−0.5	667	−0.6	258	−0.5
20	865	30	3.4	0.1	666	−0.6	257	−0.1
21	873	22	2.4	−0.9	664	−0.3	257	−0.1
22	865	30	3.3	0.0	649	2.0	252	2.1
23	906	−11	−1.3	−4.7	654	1.3	255	0.8
24	863	32	3.6	0.3	664	−0.3	257	−0.1
25	869	26	2.9	−0.4	661	0.2	254	1.1
26	863	32	3.5	0.2	661	0.2	256	0.3
27	851	44	4.9	1.7	661	0.2	255	0.6
28	869	26	2.9	−0.4	661	0.2	254	1.1
29	868	27	3.0	−0.3	661	0.2	254	1.1
30	868	27	3.0	−0.3	661	0.2	254	1.1
31	867	28	3.2	−0.1	668	−0.8	258	−0.6
Average	866	29	3.3	0	662	0	257	0
Standard deviation	17	17	1.9	2.0	15	2.3	6	2.5

TABLE VIII

Calculated (C) and Measured (E) Decay Heat Rate and Mass of ^{137}Cs and ^{148}Nd for Fuel Assembly BT04

Calculation Identification	Decay Heat Rate				^{137}Cs		^{148}Nd	
	C (W)	$E - C$ (W)	$\frac{E-C}{E}$ (%)	$\frac{\langle C\rangle - C}{\langle C\rangle}$ (%)	Mass (g)	$\frac{\langle C\rangle - C}{\langle C\rangle}$ ()]	Mass (g)	$\frac{\langle C\rangle - C}{\langle C\rangle}$ (%)
1	745	23	3.0	2.4	544	0.7	258	0.5
2	774	−6	−0.8	−1.5	546	0.4	259	0.3
3	772	−4	−0.5	−1.2	541	1.2	257	1.0
4	750	18	2.4	1.8	547	0.1	262	−1.0
5	761	7	1.0	0.3	553	−0.9	257	0.7
6	771	−3	−0.4	−1.0	550	−0.4	260	−0.1
7	734	34	4.4	3.8	544	0.6	261	−0.7
8	744	24	3.1	2.5	556	−1.6	266	−2.7
9	731	37	4.8	4.2	543	0.9	259	0.1
10	747	21	2.8	2.2	550	−0.4	261	−0.8
11	766	2	0.3	−0.4	550	−0.4	262	−0.9
12	789	−21	−2.7	−3.3	551	−0.5	259	0.1
13	809	−41	−5.3	−6.0	556	−1.5	265	−2.3
14	753	15	2.0	1.3	549	−0.3	261	−0.7
15	749	19	2.5	1.9	548	−0.1	260	−0.3
16	755	13	1.6	1.0	539	1.6	252	2.9
17	736	32	4.1	3.5	544	0.7	263	−1.2
18	761	7	0.9	0.2	550	−0.3	260	−0.3
19	767	1	0.1	−0.6	551	−0.5	260	−0.3
20	793	−25	−3.2	−3.9	551	−0.7	261	−0.5
21	768	−0	−0.0	−0.6	548	−0.1	259	0.1
22	764	4	0.6	−0.1	549	−0.2	259	0.0
23	799	−31	−4.0	−4.7	540	1.4	257	0.9
24	772	−4	−0.6	−1.2	545	0.5	257	0.9
25	766	2	0.3	−0.4	547	0.1	257	1.0
26	763	5	0.7	0.0	547	0.1	259	0.2
27	750	19	2.4	1.8	547	0.1	258	0.5
28	766	2	0.3	−0.4	547	0.1	257	1.0
29	767	1	0.1	−0.5	547	0.1	257	1.0
30	767	1	0.1	−0.5	547	0.1	257	1.0
31	769	−1	−0.2	−0.8	551	−0.5	260	−0.3
Average	763	5	0.6	0	548	0	259	0
Standard deviation	18	18	2.3	2.4	4	0.7	3	1.1

TABLE IX

Calculated (C) and Measured (E) Decay Heat Rate and Mass of ^{137}Cs and ^{148}Nd for Fuel Assembly BT05

Calculation Identification	Decay Heat Rate				^{137}Cs		^{148}Nd	
	C (W)	$E - C$ (W)	$\frac{E-C}{E}$ (%)	$\frac{\langle C\rangle - C}{\langle C\rangle}$ (%)	Mass (g)	$\frac{\langle C\rangle - C}{\langle C\rangle}$ (%)	Mass (g)	$\frac{\langle C\rangle - C}{\langle C\rangle}$ (%)
1	640	24	3.5	1.5	508	0.4	256	0.7
2	654	9	1.3	−0.8	507	0.6	256	0.4
3	652	11	1.7	−0.4	504	1.1	255	0.8
4	643	20	3.1	1.0	507	0.4	259	−0.7
5	652	11	1.7	−0.4	513	−0.7	255	1.0
6	656	7	1.1	−1.0	510	−0.1	257	0.1
7	634	29	4.4	2.4	507	0.5	259	−0.8
8	636	27	4.1	2.1	552	−8.4	282	−9.6
9	627	36	5.4	3.4	506	0.7	258	−0.2
10	632	31	4.6	2.6	510	−0.2	259	−0.6
11	651	12	1.9	−0.2	510	−0.2	259	−0.6
12	675	−12	−1.9	−4.1	511	−0.3	257	0.3
13	685	−22	−3.3	−5.6	514	−1.0	262	−1.9
14	636	27	4.0	2.0	509	0.1	258	−0.3
15	632	31	4.7	2.6	508	0.3	258	−0.2
16	646	17	2.6	0.5	513	−0.7	255	0.8
17	625	38	5.7	3.7	504	1.0	260	−0.9
18	650	13	1.9	−0.2	499	2.1	251	2.3
19	653	10	1.5	−0.6	511	−0.3	257	0.0
20	675	−12	−1.8	−4.0	510	−0.1	258	−0.3
21	653	10	1.5	−0.6	509	0.1	257	0.3
22	649	14	2.1	−0.0	509	0.0	257	0.3
23	674	−11	−1.6	−3.8	501	1.7	254	1.2
24	657	6	1.0	−1.1	506	0.7	255	1.1
25	649	14	2.1	0.0	507	0.4	254	1.4
26	647	16	2.5	0.4	507	0.4	256	0.6
27	635	28	4.3	2.2	507	0.4	255	0.8
28	649	14	2.1	0.0	507	0.4	254	1.4
29	651	12	1.7	−0.4	507	0.4	254	1.4
30	651	12	1.7	−0.4	507	0.4	254	1.4
31	654	9	1.3	−0.8	511	−0.3	258	0.0
Average	649	14	2.1	0	509	0	257	0
Standard deviation	14	14	2.1	2.2	9	1.7	5	2.0

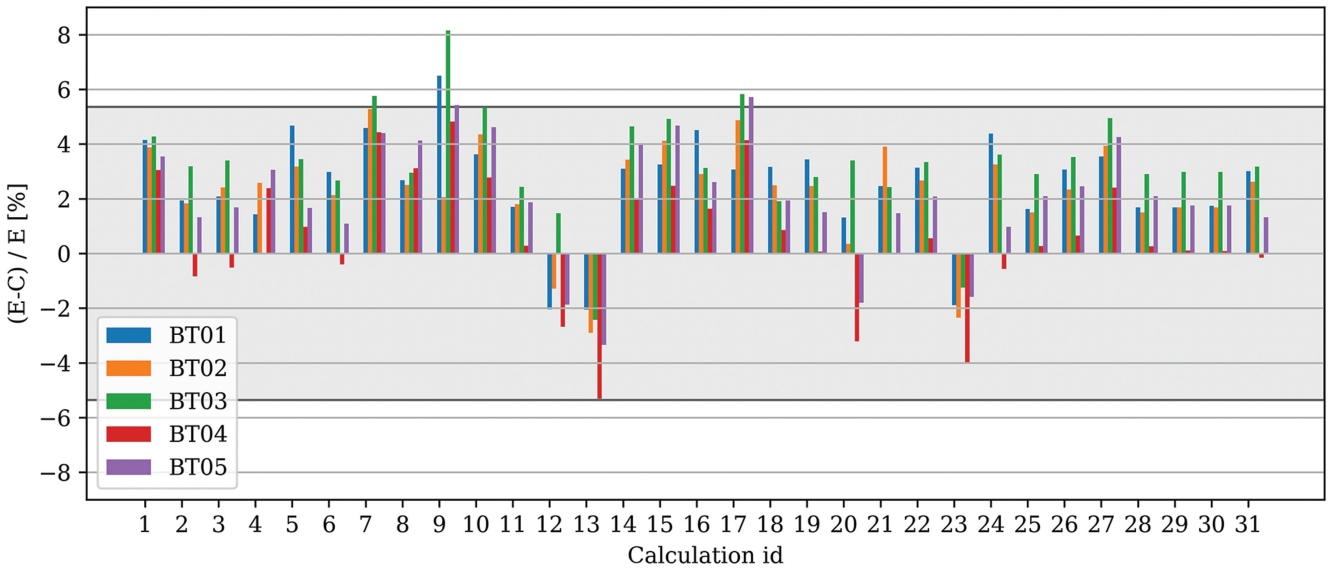

Fig. 8. Relative difference between measured (E) and calculated (C) decay heat rate values for the five different assemblies studied.

VII. SUMMARY AND CONCLUSIONS

This work has allowed for obtaining a comparison between the calculated decay heat rate values obtained by various participants, based on the same irradiation description, and validating them with measured values. This is a first-of-its-kind exercise, thanks to the openness of Vattenfall and SKB. It has led to performing a first assessment of our simulation capabilities, as well as our current prediction potentials. During this work, beyond the comparisons presented in Fig. 8, a number of questions were raised, and we were able to envisage a number of improvements for a possible follow up.

Regarding the experimental data, it is useful to recall here again the necessity of high-quality and open-source measurements, with the essential information to perform simulations. This is exactly what was available in the present case. It is of tremendous benefit for the characterization of SNF, given the scarcity of such available measurements. It was nevertheless observed that the experimental decay heat values were provided with a level of uncertainties which was in fact higher than the spread of the calculated values. Such a statement could only be made a posteriori. This indicates that, in order to improve the current predictive power, the experimental uncertainties first need to be smaller than they currently are. Consequently, experimental uncertainties smaller than 5% would be advantageous in future validation work.

It was also observed that the comparison between the experimental and calculated values seems to indicate a possible bias (i.e., systematic lower or higher calculated values, see Fig. 8). The existence of such a bias cannot be confirmed, given the uncertainty of the experimental data and the restricted experimental (and correlated) data set, but there is evidence that such an issue cannot be excluded. Additionally, the origin of such a bias is unknown, either from the simulation approach (inputs, codes, and ND), from the experimental setup, or even from both. This points out the necessity of analyzing a larger number of measurements, if possible independent from each other.

Questions also arose from the calculated schemes (inputs, assumptions, codes) and shall be studied in future work. One important and common ingredient of the various simulations is the degree of details of the irradiation history. As mentioned, a number of assumptions and simplifications were applied by the data providers. They were motivated by physical conjectures or by industrial necessities, but are nonetheless likely to be representative of "what will be available" for external parties such as waste management organizations, technical support organizations, or even safety authorities (e.g., condensed power history, availability of coastdown data). In order to assess the impact of such simplifications on calculations, it will be welcome in the future to compare calculated decay heat values based on both simplified and dense irradiation schemes. This possibly will include irradiation power as a function of cycle length, average

quantities such as fuel and moderator temperatures, void, two-dimensional (2D) versus three-dimensional (3D) representations, and other important core parameters.

As a final remark on the simulations, although the current list of remarks/questions is not exhaustive, the importance of ND was discussed during the exercise, e.g., decay data, fission yields, cross sections, or energy release. It is certainly a key quantity for the estimation of decay heat, and its impact can be partially captured by using the associated covariance information. Depending on the ND library, different "best-estimate" decay heat values can be obtained, as well as different uncertainties. This is nevertheless a partial estimation of the impact of ND, as some of them (especially for short CTs) are just not necessarily present in libraries. If not "existing" in libraries, it is also difficult to gauge their impact. A detail analysis of such impact as a function of CT would certainly be well received.

If one looks into the future and tries to take advantage of the present blind benchmark, it appears evident to answer the previous questions first. More (and better) experimental data, their in-depth analysis, and the thorough analysis of inputs, codes, assumptions, and ND are becoming the usual suspects in paving the way to our improved understanding of a quantity such as decay heat. Additionally, links between decay heat, source terms, and dose rates will help to tackle such problematic questions from a broader angle. The current exercise has been extremely profitable in defining the current and future projects, such as the European Union EURAD project (Horizon 2020) and the coordinated research project on SNF characterization from the IAEA, as well as the new working group on decay heat evaluation from the NEA/Working Party on Nuclear Criticality Safety. If one could add a request to the wish list for future open-minded industries, it would certainly be the availability of decay heat data given the amount of national proprietary programs.

VIII. OUTLOOK

In connection with this blind test, discussions were made regarding whether or not more detailed input data would give better agreement with the measurements. That is, it was suggested to compare calculations of the inventory of ^{137}Cs or ^{148}Nd based on a more detailed operational history. These discussions were not included here, but preliminary results of such calculations performed by some participants do not show any significant improvement. Further studies of the level of detail needed for input data to be able to more accurately predict the decay heat could be considered.

Similar future benchmark exercises could involve the content of more nuclides as well as comparisons of the evolution in time of the decay heat rate or nuclide inventory of the SNF.

Due to the relatively large interest in the results of this exercise, it has been suggested to follow up with an expanded study involving significantly more SNF assemblies.

APPENDIX

CODE USAGE DESCRIPTIONS

A.I. DIFFERENT PROCEDURES FOLLOWED FOR EACH CALCULATION

The following sections provide details regarding the difference procedures that were followed for each calculation. Some details on the used Q-values are given for the various codes.

A.I.A ALEPH 2.7.2 WITH ENDF/B-VII.1

The calculations were performed with the ALEPH BU code version 2.7.2 (Ref. 5) that invokes MCNP6.2 (Ref. 6) for transport calculations. ENDF/B-VII.1 general purpose, radioactive decay and fission yield libraries[7] were employed both for transport and depletion. The assembly BT03 was modeled in 3D while the others in 2D. All fuel pins were considered as a unique depletion zone. The cycles were divided into four to eight finer substeps with the boron concentration adjustment at the beginning of each substep. Each transport simulation was run for 2.5 million active neutron histories. Flux-to-power conversion was done using total energy release in all fission and capture events with recoverable energies taken from the ENDF/B-VII.1 files.

ALEPH2 employs MCNP for particle transport and thus takes advantage of detailed neutron balance table. Statistical neutron weights lost to capture and fission on all nuclides involved in the problem are multiplied by the corresponding fission and capture recoverable energies to get the total energy release. Fission (total release less the neutrino energy) and capture Q-values are taken from the ND library, i.e., ENDF/B-VII.1 used for blind test calculations. Explicit calculation of energy release in neutron capture reactions allows accurate treatment of the

problems where the contribution of these reactions into the energy balance becomes substantial, as in the BT03 case with Gd BA.

A.I.B. APOLLO2.8/DARWIN2.3 WITH JEFF-3.1.1

The DARWIN2.3 code system[89] is devoted to the characterization of SNFs. It includes the 2D neutron transport code APOLLO2 (Ref. 10) that generates accurate reaction rates as a function of BU and the PEPIN2 code that solves the Bateman equations with a detailed irradiation history and almost complete decay chains (about 3800 isotopes). Calculations are performed with the JEFF-3.1.1 library.[1112] DARWIN2.3 is validated upon a large experimental database of post-irradiated examinations and integral decay heat experiments.[9]

A.I.C. CASMO-4E-2.2 + ORIGEN-S WITH JEF-2.2

This calculation methodology consists of CASMO-4E BU calculation using the 70-group JEF-2.2 library followed by ORIGEN-S decay calculation. The isotopic concentrations at the end of irradiation are calculated with CASMO-4E using the default BU step sizes and division of burnable regions. The isotopic concentrations at the end of irradiation are used in the ORIGEN-S decay calculation that computes the spent fuel properties such as isotopic concentrations, activities, and decay heat after given CT.

A.I.D. CASMO-5 (2.03) WITH ENDF/B-VII.1

The nominal calculations were performed with CASMO-5, version 2.03 (Ref. 13), using the ENDF/B-VII.1 library (called e7r1.201.586.bin in CASMO) (Ref. 7). The input file model follows the CASMO-5 structure that was used to analyze the Paul Scherrer Institute PROTEUS phase II samples without sample relocation: four steps per cycle; defining the sample power, fuel, and moderator temperature; the boron concentration; and the depletion step. The isotope concentrations after final shutdown and cooling were obtained with the option SNF light option of CASMO. For the calculations of uncertainties other than ND, the same CASMO version and inputs were used, randomly changing the previous quantities. A number of random calculations were performed, providing standard deviations (uncertainties) on isotopic concentrations and other quantities. Concerning the propagation of uncertainties due to ND, a modified version of CASMO-5, version 2.03, was used, called SHARK-X, where random cross sections are used instead of the nominal ones. These random cross sections are produced based on the ENDF/B-VII.1 covariance library.

The default approach in CASMO-5 to calculating the energy release for capture is to use the constants based on Ref. 14. The fission energy release model, not required for neutron transport, is used for determining the BU rate (constant flux approximation). Details can be found in Ref. 15. In the case of the main actinides, the fission and total Q-values are listed as follows:

1. ^{235}U: Q_{fission} = 193.41 MeV and Q_{total}[b] = 202.30 MeV
2. ^{238}U: Q_{fission} = 197.79 MeV and Q_{total} = 206.70 MeV
3. ^{239}Pu: Q_{fission} = 198.90 MeV and Q_{total} = 211.20 MeV
4. ^{241}Pu: Q_{fission} = 201.98 MeV and Q_{total} = 213.60 MeV.

A.I.E. CASMO-5 (2.12.00)/SNF (1.07.02)

This methodology combines isotopic concentrations, fluxes, and cross sections calculated by the neutron transport and depletion code CASMO-5 with irradiation history data and tabulated isotopic decay data.[716] These data sources are used and processed by the SNF code to compute the SNF characteristics, including the decay heat power. The code's distributable versions are applied to the provided input data without modifications. The end-of-life assembly BUs [megawatt days/tonnes heavy metal (HM)] are determined by summation of the cycle BU computed as (assembly power in megawatts) multiplied by (time in power in days) divided by [initial HM mass in tonnes].

A.I.F. DRAGON 4.0.5 WITH SHEM-295 BASED ON ENDF/B-VII.1

These calculations were performed using DRAGON 4, version 4.0.5. A one-level scheme using the interface current method was chosen for both the self-shielding and main flux calculation. The self-shielded ENDF/B-VII.1-

[b] Q_{total} does not include the neutrino energy.

based SHEM-295 cross sections[7,17] were prepared using a subgroup approach, where the fuel region was divided into four annular rings with the following volumes: 50%, 30%, 15%, and 5%. Two-dimensional calculation in infinite assembly lattice was applied. All fuel pins were treated as one depletion mixture.

In the DRAGON code, the EVO module performs the BU calculations. The constant power normalization technique was used to obtain the solution of depletion equations. In this case, the power released per initial heavy element at beginning of stage and end of stage is set to a constant value. In addition, the energy released outside the fuel was determined using the GLOB option. The energy released by fission in the DRAGON code is determined with the *H*-factor, which is used to calculate the recoverable energy from fission reactions. The *H*-factor or groupwise energy production coefficients H^g are a product of each microscopic fission cross section times the energy emitted by specific reaction κ. The Q-values are taken from the depletion chain data listed in the used nuclear library. Some values for fission, taken from the applied ENDF/B-VII.1 library, are listed as follows:

1. ^{235}U: 192.21 MeV
2. ^{238}U: 196.28 MeV
3. ^{239}Pu: 197.83 MeV.

A.I.G. EVOLCODE (MCNP + ACAB) WITH JEFF-3.3

The simulation has been performed with the EVOLCODE system[18] using the JEFF-3.3 data library for cross-section[19,20] decay data (including heat emission), isomer branching ratios, and fission yields. These specifications also included the BU history, described in the simulations with irradiation steps of 10 and 40 days for the beginning of each cycle and general steps of 50 days for the rest of the irradiation.

The energy released by fission in EVOLCODE is considered to be totally deposited in the place where the fission occurs, so the power in the neutronics process is driven by the Q-values present in the MCNP source code, which are based on ENDF/B-VI. However, the depletion process is done by ACAB, which uses an expression for the recoverable energy per fission that depends on the atomic number and the mass number of the fissioning actinide (following a semi-empirical formula from Ref. 21). Due to this, EVOLCODE uses a predictor/corrector method to solve this inconsistency so that the neutron flux in the depletion process is modified so that the irradiation has the thermal power specified by the user.

A.I.H. MCNP-CINDER + NUKLEONIKA (2D)

The calculations performed used the MCNP6.1 code coupled with the CINDER BU module. The Bateman equation is solved based on a linearization approach[22] used in CINDER. The BU process is done by using 69 energy groups, which differs from the "classical" one-group Bateman equation exponential solution. Further, in this study it was shown that for the MCNP-CINDER linear solver, the BU day numbers should be limited to about 50. The (2D) symbol indicates that for the BT03 Gd case, the full length of the rod according to the specification was introduced, which enhanced to some extent the inaccuracy due to additional statistical uncertainties. The decay heat calculations were done by transferring the decaying nuclide vector to the Nucleonica program, in which the decay heat includes isomers in a better manner and the heat is introduced with its decay radiation type.[7,22–27]

A.I.I. MONTEBURNS V3 + CINDER WITH ENDF/B-VII.1

Monteburns v3, which links the Monte Carlo transport code MCNP6.1 with the isotope generation and depletion code CINDER90 (Refs. 28 and 29), was used for these calculations. MCNP/Monteburns input files for neutron transport and irradiation of each of the five assemblies of interest were generated and calculations were performed over 34 to 36 different individual time steps, varying the soluble boron concentration during each step (and cycle), as given in the input definition. Albedo boundary conditions on an infinitely reflected assembly model in MCNP were used to simulate the contribution of surrounding assemblies. For CINDER, the Q-values are 202.61 and 211.41 MeV for ^{235}U and ^{239}Pu, respectively.[30]

A.I.J. MOTIVE (KENO-VI + VENTINA) WITH ENDF/B-VII.1

The calculations were performed using KENO-VI from SCALE 6.2.2 as the external Monte Carlo code and Ventina as the depletion code.[31,32] ENDF/B-VII.1 library data[7] were used for both transport and depletion calculations. All fuel assemblies were modeled using an effective 2D model with single depletable material, i.e., the same fuel material in all pins, and one fuel zone per pin, except for BT03 where for the Gd-rod the ten fuel ring zones were

applied with separate depletable materials. The cycles were subdivided into time steps of 50 days interpolating the coolant boron content to each of the time steps and using a standard predictor-corrector approach. The fission energy calculation is done explicitly taking into account all fission and capture events with their respective recoverable energies as provided by the data library.

A.I.K. MOTIVE (OPENMC + VENTINA) WITH ENDF/B-VIII

This is the same as Sec. A.I.J except that OpenMC version 0.9.0 (Ref. 33) was used as the Monte Carlo neutron transport code in conjunction with ENDF/B-VIII data[27] for both transport and depletion.

A.I.L. MVP3 WITH ENDF/B-VII.1

This is the same procedure as in Sec. A.I.N except that the ENDF/B-VII.1 library[7] was used for the reaction rate calculation.

A.I.M. MVP3 WITH JEFF-3.2

This is the same procedure as in Sec. A.I.N except that the JEFF-3.2 library[34] was used for the reaction rate calculation.

A.I.N. MVP3 WITH JENDL-4.0

Two-dimensional assembly calculations were performed with MVP3 (Ref. 35) using the JENDL-4.0 library.[36] MVP3 is a continuous-energy Monte Carlo code coupled with a BU solver developed by the Japan Atomic Energy Agency. Twenty-four million neutrons were employed in an active run to tally the reaction rate in each BU step. In the depletion calculations, the detailed BU chain of ChainJ40 (Ref. 37) (named th2cm6fp193bp8T_J40 in ChainJ40) and the predictor-corrector option were applied to obtain the isotopic composition in the burnt fuel. The deposition energy per fission used in ChainJ40 are 202.25, 205.92, 210.96, and 213.27 MeV for ^{235}U, ^{238}U, ^{239}Pu, and ^{241}Pu, respectively. The decay heat was deduced by the products of the composition, the decay constant, and the energy release per decay. The data related to the radioactive decay were taken from JENDL/DDF-2015 (Ref. 38).

A.I.O. OREST WITH JEF-2.2 FOR CROSS SECTIONS AND ENDF/B-VI FOR DECAY DATA

In OREST, the flux calculation is performed by a one-dimensional deterministic transport solver on an effective circular pin cell with the cell radius adjusted such that it reflects the moderation ratio of the fuel assembly to be modeled. For the calculation, a data library based on JEF-2.2 (neutron transport) and ENDF/B-VI (depletion) was used.[39] The cycles were subdivided into time steps of 50 days interpolating the coolant boron content to each of the time steps. No predictor-corrector approach was used, however, the chosen time steps are automatically subdivided into finer steps by the code. The fission energy calculation is done explicitly taking into account all fission and capture events with their respective recoverable energies as provided by the data library. For BT03 an effective 2D model similar to that applied in the MOTIVE cases was used by applying the code KENOREST, which couples OREST to the multigroup Monte Carlo code KENO-Va (SCALE 4.4a).

A.I.P. SCALE 6.0: ORIGEN-ARP WITH ENDF/B-V AND SCALE 6.2.3: ORIGAMI WITH ENDF/B-VII.1

In the SCALE 6.0/ORIGEN-ARP (Ref. 40) and SCALE 6.2.3/ORIGAMI (Ref. 41) cases, standard and pregenerated one-group libraries of 17 × 17 (Westinghouse) fuel assemblies were used, fixed water density was assumed, and the average boron concentration, fixed moderator temperature, and only average assembly power were used for modeling. The cladding material in ORIGEN-ARP was used as exists in standard pregenerated one-group libraries (Zircaloy-2 for 17 × 17 assemblies). The cladding and spacer material concentrations and impurities in ORIGAMI were used as in Ref. 42. The ORIGAMI calculations were performed in single-assembly mode with no full-core calculation (i.e., no position-sensitive cases were analyzed). The calculations were run using ENDF/B-V (Ref. 43) and ENDF/B-VII.1 (Ref. 7) (respectively, for SCALE 6 and SCALE 6.2.3 versions) based cross section, radioactive decay, and fission yield data libraries, which are validated for PWR-type SNF calculation.[4445] The BU calculation was run using a standard predictor-corrector algorithm and ten steps per cycle. The ^{235}U Q-value for fission according to SCALE documentation is 194.02 MeV, taken from ENDF/B-VII.1 evaluations.

A.I.Q. SCALE 6.1.3: ORIGEN-ARP WITH ENDF/B-V

ORIGEN-ARP (Ref. 40) was used to run calculations based on ORIGEN under SCALE 6.1.3. The standard

Westinghouse 17 × 17 libraries for ORIGEN-ARP, as distributed with SCALE 6.1.3 (Ref. 43), were used through the Express Form interface with a standard moderator density and defining only the main ^{235}U enrichment. The input information was comparable to the set of data normally requested during safeguards inspections on spent fuel. Therefore, the simulation did not include a detailed core layout with the actual positions of the fuel assemblies during the different cycles and exact burnable poison content.

A.I.R. SCALE 6.2.3: POLARIS, ORIGEN, AND TRITON/NEWT WITH ENDF/B-VII.1

The calculations were performed using the Polaris, ORIGEN, and TRITON codes of the SCALE code system version 6.2.3 (Ref. 41). The ND are SCALE cross sections, fission yields, and decay data based on ENDF/B-VII.1 ND (Ref. 7). The TRITON and Polaris models use the SCALE multigroup library of the 56-group structure. The ORIGEN models use one-group libraries at mid-BU values generated by TRITON for the 17 × 17 lattice and using also the ARP cross-section interpolation utility. The TRITON and Polaris models are 2D models of the southeast quarters of the assemblies along with reflective boundary conditions, and the ORIGEN models are zero dimensional. One depletion and decay model was made for each assembly, except for the BT03 assembly which was modeled using two 2D models for the BA section and the BA-free sections. The Polaris models deplete each pin individually, the TRITON models deplete the lattice into three individual materials, and the ORIGEN models deplete a single material. Only the BA rods of the BT03 assembly were radially divided into eight individual depletion zones. The BU calculations implement the predictor-corrector method, along with four to six substeps per cycle. The activation and decay heat from the cladding and the spacers were accounted for in all models. The spacers were included in the models as extra cladding thickness.

A.I.S. SCALE 6.2.3: TRITON/KENO WITH ENDF/B-VII.1

The calculations were performed using the TRITON sequence of SCALE 6.2.3 (Ref. 41), coupling the ORIGEN module with KENO-V.a with multigroup option using ENDF/B-VII.1-based cross sections.[7] The same ND library was used for the nuclide inventory calculations with ORIGEN. In this study, coarse time steps of 50 days were adopted, except for the first few time steps which were much shorter to accommodate the rapid changes in fission product concentrations.

A.I.T. SCALE 6.2.3: TRITON/NEWT WITH ENDF/B-VII.1

Depletion simulations were performed for each assembly with TRITON/NEWT in SCALE version 6.2.3 (Ref. 41) and 252-group ENDF/B-VII.1 cross-section data.[7] Both the fuel and the cladding were considered depleted mixtures. Spacers were not included in the TRITON model. The effect of the spacers on assembly decay heat at these CTs is expected to be negligible for the type of spacers applicable to the studied assemblies, which have no or a very small amount of Co impurity content. The effect of the spacers' inclusion in the assembly decay heat is less than 0.1 W, as estimated with the ORIGAMI graphical user interface for ORIGEN.

Both the recoverable energy contributed by fission and that by capture are accounted for in the calculation. The recoverable energy values are taken primarily from ENDF/B-VII.1 evaluations. Nuclide-specific Q-fission and Q-capture are applied for 24 actinides (isotopes of Th, Pa, Np, U, Pu, Am, and Cm) as available from ENDF/B-VII.1, whereas for other actinides a 200-MeV value is assumed. Nuclide-specific Q-capture values are used for 32 fission and activation products as taken from ENDF/B-VII.1, and for other nuclides a 5.0-MeV is assumed, see Ref. 46.

A.I.U. SEADEP WITH JEFF-3.1.1

SEADEP is a calculation methodology based on the use of the MONTEBURNS 2.0 (Ref. 29) calculation system, which is based on Monte Carlo transport code MCNPX and depletion code ORIGEN (Ref. 24). The use of the code has been modified as necessary to obtain the results of residual heat of the most significant nuclides. The contribution of ^{85}Kr and of other nuclides not having treatment in SEADEP have been estimated by calculation with SCALE 6.1. The residual heat due to the activation of the structural components of the fuel assembly has been calculated with SCALE 4.4.

The SEADEP methodology is oriented to a detailed representation of the sample to be cut, dissolved, and finally measured. Therefore, the irradiation conditions are specific for that small fraction of the fuel rod. The rest of the fuel rod containing the sample and the rest of the assembly are represented in an ad hoc manner according to experience and always trying to provide realistic conditions in terms of degree of moderation (presence of guide tubes, assembly gap, core baffle, etc.), in terms of leakage (end of fuel assembly, core periphery, etc.), and in terms of water density, boron content, and fuel temperature.

The MONTEBURNS uses a user-provided value for the fission energy deposited by the fission of ^{235}U and tabulated values relative to it for the other fissionable nuclides. The manual-recommended value of 200 MeV for ^{235}U was used in the calculations.

A.I.V. SERPENT 2.1.29 WITH ENDF/B-VII.1

The calculations were run using Serpent version 2.1.29, with ENDF/B-VII.1-based cross-section libraries,[7] radioactive decay, and fission yield data. All models were 2D, except the BT03 model, which was 3D. All fuel pins in the assembly model were treated in the same depletion zone, with each pin divided in four equivolume radial zones. The BU calculation was run using a standard predictor-corrector algorithm and four to eight steps per cycle. A total of 2.5 million active neutron histories were run per each transport simulation. Normalization was fixed by setting the energy deposited per ^{235}U fission to 202.27 MeV.

A.I.W. SERPENT 2.1.29 WITH JEFF-3.1.1

The calculations were performed using released Serpent 2.1.29 (Ref. 47) coupled to JEFF-3.1.1 libraries (cross sections, fission yields, and decay data). All fuel pins in the assembly model were treated in the same depletion zone, with each pin divided in three equivolume radial zones. An average boron concentration (middle of cycle value) was taken per cycle. The BU calculation was run using a standard predictor-corrector algorithm with 14 to 17 steps per power operation cycle. A total of 2.8 million active neutron histories were run per each transport simulation. Normalization was fixed by setting the energy deposited per ^{235}U fission to 202.27 MeV.

A.I.X. SERPENT 2.1.31 WITH JEFF-3.2-BASED CROSS-SECTION LIBRARIES AND JEFF-3.1.1-BASED RADIOACTIVE DECAY AND FISSION YIELD DATA

The calculations were run using development version Serpent 2.1.31 (Ref. 47), with JEFF-3.2-based cross-section libraries and JEFF-3.1.1-based radioactive decay and fission yield data. Each fuel pin was treated as a separate depletion zone and divided radially into a central zone and a 0.3-mm-thick surface layer. The BU calculation was run using a standard predictor-corrector algorithm and 50 steps per cycle. A total of 10 million neutron histories were run per each transport simulation. Normalization was fixed by setting the energy deposited per ^{235}U fission to 202.27 MeV.

The fission Q-values provided in the ACE data format do not represent the deposited energy, mainly because the secondary energy released in the capture of fission neutrons is omitted. By default, Serpent uses a fixed value of 202.27 MeV for the fission energy deposition of ^{235}U. The values for other nuclides are scaled based on this value, and the ratio of the tabulated Q-value and that of ^{235}U. It is possible to override the fission energy deposition of any nuclide by user input. Serpent also provides advanced energy deposition modes, which explicitly take into account the contribution of fission neutrons, as well as photons produced in neutron interactions.[48] These modes, however, were not applied in this study.

Acknowledgments

The staff at the Ringhals nuclear power plant in Sweden are acknowledged for providing input data for this exercise. The OECD/NEA and JRC-Geel are acknowledged for hosting the meetings. The SKB documents, i.e., Refs. 2 and 3, will be submitted on request to document@skb.se.

Disclosure Statement

No potential conflict of interest was reported by the author(s).

ORCID

Peter Jansson http://orcid.org/0000-0002-3136-5665
Ulrika Bäckström http://orcid.org/0000-0003-2040-5366
Francisco Álvarez-Velarde http://orcid.org/0000-0002-2050-0550
Stefano Caruso http://orcid.org/0000-0003-1424-5116
Lydie Giot http://orcid.org/0000-0001-9764-5005
Kevin Govers http://orcid.org/0000-0003-2196-3124
Augusto Hernandez Solis http://orcid.org/0000-0002-7439-1994
Marjan Kromar http://orcid.org/0000-0001-8960-203X
Jaakko Leppänen http://orcid.org/0000-0003-1907-2883
Rita Plukienė http://orcid.org/0000-0003-2394-4760
Dimitri Rochman http://orcid.org/0000-0002-5089-7034
Peter Schillebeeckx http://orcid.org/0000-0002-1181-4144
Holly Trellue http://orcid.org/0000-0003-2051-0852

References

1. P. JANSSON et al., "Data from Calorimetric Decay Heat Measurements of Five Used PWR 17 × 17 Nuclear Fuel

Assemblies," *Data Br.*, **28**, 104917 (2020); https://doi.org/10.1016/j.dib.2019.104917.

2. P. JANSSON, "KBP6003 Methodology for Uncertainty Analysis of Calorimetric Measurement with the Temperature Rising Method," SKB Document 1533630, v3.0, Swedish Nuclear Fuel and Waste Management Company (2021).
3. M. BENGTSSON and P. JANSSON, "KBP6003—Methodology for Assessment of Calorimetric Measurement with the Temperature Rising Method," SKB Document 1629283, v 4.0, Swedish Nuclear Fuel and Waste Management Company (2020).
4. "Measurements of Decay Heat in Spent Nuclear Fuel at the Swedish Interim Storage Facility, Clab," R-05-62, Swedish Nuclear Fuel and Waste Management Company (2006); https://www.skb.se/publikation/1472024/R-05-62.pdf (current as of Oct. 5, 2021).
5. A. STANKOVSKIY and G. VAN DEN EYNDE, "Advanced Method for Calculations of Core Burn-Up, Activation of Structural Materials, and Spallation Products Accumulation in Accelerator-Driven Systems," *Sci. Technol. Nucl. Ins.*, **2012**, 1 (2012); https://doi.org/10.1155/2012/545103.
6. C. J. WERNER et al., "MCNP Version 6.2 Release Notes," LA-UR–18-20808, 1419730, Los Alamos National Laboratory (2018); https://doi.org/10.2172/1419730.
7. M. CHADWICK et al., "ENDF/B-VII.1 Nuclear Data for Science and Technology: Cross Sections, Covariances, Fission Product Yields and Decay Data," *Nucl. Data Sheets*, **112**, *12*, 2887 (2011); https://doi.org/10.1016/j.nds.2011.11.002.
8. A. TSILANIZARA et al., "DARWIN: An Evolution Code System for a Large Range of Applications," *J. Nucl. Sci. Technol.*, **37**, *Sup1*, 845 (2000); https://doi.org/10.1080/00223131.2000.10875009.
9. L. SAN-FELICE, R. ESCHBACH, and P. BOURDOT, "Experimental Validation of the DARWIN2.3 Package for Fuel Cycle Applications," *Nucl. Technol.*, **184**, *2*, 217 (2013); https://doi.org/10.13182/NT12-121.
10. A. SANTAMARINA et al., "APOLLO2.8: A Validated Code Package for PWR Neutronics Calculations," presented at the ANFM 2009, Hilton Head Island, South Carolina, April 12–15 (2009).
11. A. SANTAMARINA et al., "The JEFF-3.1.1 Nuclear Data Library. JEFF Report 22—Validation Results from JEF-2.2 To JEFF-3.1.1," OECD 2009 NEA No. 6807, p. 62, Nuclear Energy Agency (2009); https://www.oecd-nea.org/upload/docs/application/pdf/2019-12/nea6807-jeff22.pdf (current as of Oct. 5, 2021).
12. M. A. KELLETT, O. BERSILLON, and R. W. MILLS, "The JEFF-3.1/-3.1.1 Radioactive Decay Data and Fission Yields Sub-libraries. JEFF Report 20," OECD 2009 NEA No. 6287, p. 148, Nuclear Energy Agency (2009); https://www.oecd-nea.org/upload/docs/application/pdf/2019-12/nea6287-jeff-20.pdf (current as of Oct. 5, 2021).
13. J. RHODES, K. SMITH, and D. LEE, "CASMO-5 Development and Applications," presented at the PHYSOR-2006 Conf. ANS Topl. Mtg. on Reactor Physics, American Nuclear Society, Vancouver, British Columbia, Canada, September 10–14 (2006); http://inis.iaea.org/search/search.aspx?orig_q=RN:43130064 (current as of Oct. 5, 2021).
14. A. PERSIC and A. TRKOV, "The Energy Released by Neutron Capture in Thermal Reactors," 83-90, Nuclear Society of Slovenia (1999); http://inis.iaea.org/search/search.aspx?orig_q=RN:33071002 (current as of Oct. 5, 2021).
15. J. RHODES, K. SMITH, and Z. XU, "CASMO-5 Energy Release per Fission Model," Paul Scherrer InstitutPSI, Switzerland (2008); http://inis.iaea.org/search/search.aspx?orig_q=RN:41119081 (current as of Oct. 5, 2021).
16. T. SIMEONOV and C. WEMPLE, "Update and Evaluation of Decay Data for Spent Nuclear Fuel Analyses," *EPJ Web Conf.*, **146**, 4 (2017); https://doi.org/10.1051/epjconf/201714609011.
17. A. HÉBERT, "Development of the Subgroup Projection Method for Resonance Self-Shielding Calculations," *Nucl. Sci. Eng.*, **162**, *1*, 56 (2009); https://doi.org/10.13182/NSE162-56.
18. F. ÁLVAREZ VELARDE, E. GONZÁLEZ-ROMERO, and I. M. RODRÍGUEZ, "Validation of the Burn-up Code EVOLCODE 2.0 with PWR Experimental Data and with a Sensitivity/Uncertainty Analysis," *Ann. Nucl. Energy*, **73**, 175 (2014); https://doi.org/10.1016/j.anucene.2014.06.049.
19. "The JEFF-3.3 Release," OECD/NEA Data Bank, Organisation for Economic Co-operation and Development/Nuclear Energy Agency (2017); http://www.oecd-nea.org/dbdata/jeff/jeff33/ (current as of Oct. 5, 2021).
20. A. J. M. PLOMPEN et al., "The Joint Evaluated Fission and Fusion Nuclear Data Library, JEFF-3.3," *Eur. Phys. J. A*, **56**, *7*, 181 (2020); https://doi.org/10.1140/epja/s10050-020-00141-9.
21. J. P. UNIK and J. E. GINDLER, "Critical Review of the Energy Released in Nuclear Fission," ANL–7748, Argonne National Laboratory (1971); https://doi.org/10.2172/4010075.
22. W. WILSON, T. ENGLAND, and K. VAN RIPER, "Status of CINDER90 Codes and Data," *Proc. IV SARE Workshop*, T. A. GABRIEL, Ed., p. 69, Knoxville, Tennessee, September 14–16 (1998).
23. F. B. BROWN, "Doppler Broadening Resonance Correction for Free-Gas Scattering in MCNP6.2," LA-UR–19-24824, 1523218, Los Alamos National Laboratory (2019); https://doi.org/10.2172/1523218.
24. A. CROFF, "User's Manual for the ORIGEN2 Computer Code," ORNL/TM-7175, 5285077, Oak Ridge National Laboratory (1980); https://doi.org/10.2172/5285077.

25. H. R. TRELLUE, M. L. FENSIN, and J. D. GALLOWAY, "Production and Depletion Calculations Using MCNP," presented at the MCNP/ENDF/NJOY Workshop, 22, Los Alamos, New Mexico, October 30 - November 1 (2012); https://mcnp.lanl.gov/pdf_files/la-ur-12-25804.pdf (current as of Oct. 5, 2021).

26. P. COSGROVE, E. SHWAGERAUS, and G. PARKS, "Neutron Clustering as a Driver of Monte Carlo Burn-up Instability," *Ann. Nucl. Energy*, **137**, 106991 (2020); https://doi.org/10.1016/j.anucene.2019.106991.

27. D. BROWN et al., "ENDF/B-VIII.0: The 8th Major Release of the Nuclear Reaction Data Library with CIELO-Project Cross Sections, New Standards and Thermal Scattering Data," *Nucl. Data Sheets*, **148**, 1 (2018); https://doi.org/10.1016/j.nds.2018.02.001.

28. H. R. TRELLUE and P. M. MENDOZA, "Decay Heat Calculations for Blind Test," Report LA-UR-18-31774, Los Alamos National Laboratory (2019).

29. H. R. TRELLUE and D. I. POSTON, "User's Manual, Version 2.0 For MONTEBURNS, Version 5B," Report LA-UR-99-4999, Los Alamos National Laboratory (1999).

30. W. B. WILSON et al., "Recent Development of the CINDER'90 Transmutation Code and Data Library for Actinide Transmutation Studies," LA-UR-95-2181; CONF-9509162-5, Los Alamos National Laboratory (1995); https://www.osti.gov/biblio/102215 (current as of Oct. 5, 2021).

31. V. HANNSTEIN, M. BEHLER, and F. SOMMER, "Towards a Validation of the Burn-up Code Motive," presented at PHYSOR 2018: Reactor Physics Paving the Way Towards More Efficient Systems, Q. R., Mexico, April 22–26 (2018); http://inis.iaea.org/search/search.aspx?orig_q=RN:50006182 (current as of Oct. 5, 2021).

32. V. HANNSTEIN, M. BEHLER, and F. SOMMER, "Validation of the Burn-Up Code MOTIVE Using ENDF/B-VIII Data," presented at the ICNC 2019. Int. Conf. on Nuclear Criticality Safety, Paris, France, September 15–20 (2019).

33. P. K. ROMANO et al., "OpenMC: A State-of-the-Art Monte Carlo Code for Research and Development," *Ann. Nucl. Energy*, **82**, 90 (2015); https://doi.org/10.1016/j.anucene.2014.07.048.

34. "JEFF-3.2 Evaluated Data Library—Neutron Data," OECD/NEA Data Bank, Organisation for Economic Co-operation and Development/Nuclear Energy Agency (2014); https://www.oecd-nea.org/dbforms/data/eva/evatapes/jeff_32/ (current as of Oct. 5, 2021).

35. Y. NAGAYA et al., "MVP/GMVP Version 3: General Purpose Monte Carlo Codes for Neutron and Photon Transport Calculations Based on Continuous Energy and Multigroup Methods," JAEA-Data/Code 2016-018, Japan Atomic Energy Agency (2017); https://doi.org/10.11484/jaea-data-code-2016-018.

36. K. SHIBATA et al., "JENDL-4.0: A New Library for Nuclear Science and Engineering," *J. Nucl. Sci. Technol.*, **48**, *1*, 1 (2011); https://doi.org/10.1080/18811248.2011.9711675.

37. K. OKUMURA, K. KOJIMA, and T. OKAMOTO, "Development of the Burn-up Chain Data ChainJ40 Based on JENDL-4.0," presented at the *Annual Mtg. Atomic Energy Soc. of Japan.*, pp. 145–145, Japan, March 27 (2012); https://doi.org/10.11561/aesj.2012s.0.145.0.

38. J.-I. KATAKURA and F. MINATO, "JENDL Decay Data File 2015," Japan Atomic Energy Agency (2016); https://doi.org/10.11484/jaea-data-code-2015-030.

39. U. HESSE et al., "LWR Decay Heat Calculations Using a GRS Improved ENDF/B-VI Based ORIGEN Data Library," ND2007, 224, EDP Sciences, Nice, France (2007); https://doi.org/10.1051/ndata:07480.

40. I. GAULD et al., "ORIGEN-ARP: Automatic Rapid Processing for Spent Fuel Depletion, Decay, and Source Term Analysis," ORNL/TM–2005/39, Version 6, p. 1, Oak Ridge National Laboratory (2006).

41. B. T. REARDEN and M. A. JESSEE, "SCALE Code System," ORNL/TM–2005/39 Version 6.2.3, Oak Ridge National Laboratory (2018); https://doi.org/10.2172/1426571.

42. D. MENNERDAHL, "Assessment of PWR Fuel Depletion and of Neutron Multiplication Factors for Intact PWR Fuel Copper Canisters—Main Review Phase," 2013:16, Swedish Radiation Safety Authority (2013); https://www.stralsakerhetsmyndigheten.se/contentassets/54adbd7928ff406c8d3cad9a07fbed1f/201316-technical-note-assessment-of-pwr-fuel-depletion-and-of-neutron-multiplication-factors-for-intact-pwr-fuel-copper-canisters–main-review-phase (current as of Oct. 5, 2021).

43. R. KINSEY, "ENDF/B Summary Documentation," BNL-NCS-17541(Ed.3), ENDF-201(Ed.3), Brookhaven National Laboratory (1979); https://doi.org/10.2172/5405390.

44. G. ILAS, I. GAULD, and V. JODOIN, "LWR Cross Section Libraries for ORIGEN-ARP in SCALE 5.1," *Trans. Am. Nucl. Soc.*, **95**, 706 (2006).

45. G. ILAS, I. C. GAULD, and G. RADULESCU, "Validation of New Depletion Capabilities and ENDF/B-VII Data Libraries in SCALE," *Ann. Nucl. Energy*, **46**, 43 (2012); https://doi.org/10.1016/j.anucene.2012.03.012.

46. W. WIESELQUIST, R. LEFEBVRE, and M. JESSEE, "SCALE Code System," ORNL/TM–2005/39 Version 6.2.4, Oak Ridge National Laboratory (2020); https://doi.org/10.2172/1616812.

47. J. LEPPÄNEN et al., "The Serpent Monte Carlo Code: Status, Development and Applications in 2013," *Ann. Nucl. Energy*, **82**, 142 (2015); https://doi.org/10.1016/j.anucene.2014.08.024.

48. R. TUOMINEN, V. VALTAVIRTA, and J. LEPPÄNEN, "New Energy Deposition Treatment in the Serpent 2 Monte Carlo Transport Code," *Ann. Nucl. Energy*, **129**, 224 (2019); https://doi.org/10.1016/j.anucene.2019.02.003.